Polarized tops from stop decays at the LHC

JHEP03(2009)141

(http://iopscience.iop.org/1126-6708/2009/03/141)

JHEP

Published by IOP Publishing for SISSA

Received: *January 7, 2009*
Accepted: *February 26, 2009*
Published: *March 30, 2009*

Polarized tops from stop decays at the LHC

Maxim Perelstein and Andreas Weiler

Institute for High Energy Phenomenology,
Newman Laboratory of Elementary Particle Physics,
Cornell University, Ithaca, NY 14853, U.S.A.

E-mail: mp325@cornell.edu, aw288@cornell.edu

Abstract: In supersymmetric models, scalar top quarks, or stops, generically have parity-violating couplings to top quarks. As a result, tops produced in stop decays should be polarized. In this paper, we will argue that this effect may be observable at the LHC with realistic integrated luminosities, provided that one of the stops is copiously produced and can decay to a top and a neutralino. We define the "effective" stop mixing angle, which determines the degree of top polarization, and discuss the prospects for a measurement of this angle at the LHC. If some information about the neutralino mixing matrix is available, this measurement can be used to constrain the mixing angle in the stop sector, one of the most important ingredients in assessing the naturalness of electroweak symmetry breaking in the MSSM.

Keywords: Supersymmetric Standard Model, Hadronic Colliders

ArXiv ePrint: 0811.1024

doi:10.1088/1126-6708/2009/03/141

JHEP03(2009)141

Contents

JHEP03(2009)141

1 Introduction

Supersymmetric (SUSY) extensions of the Standard Model (SM) are one of the most compelling candidates for physics at the electroweak scale [1, 2]. Among many new particles predicted by these models, scalar partners of the top quark, the stops $\tilde{t}_1$ and $\tilde{t}_2$, play a special role. The reason is that the top Yukawa coupling is by far the strongest coupling of the SM Higgs. The dominant quantum contributions to the Higgs potential arise from loops of the top quark and its superpartners. These contributions play an important role in the physics of electroweak symmetry breaking (EWSB) in this framework. For example, in no-scale unified models such as mSUGRA, they are responsible for triggering EWSB by driving the Higgs mass^2 term negative, while all other scalar masses remain real. More generally, the stop and top loops give a sizeable contribution to the parameters determining the EWSB scale and the Higgs mass spectrum. Thus, if TeV-scale SUSY is realized in nature and discovered at the LHC, determining the properties of the stop quarks will be crucial in understanding the mechanism of EWSB.

In the minimal supersymmetric standard model (MSSM), sizable quantum corrections to the physical mass of the lightest CP-even Higgs are required to satisfy the LEP-2 lower bound on this mass [3]. The tension between this requirement and naturalness of the EWSB scale is known as the "LEP paradox" or "little hierarchy problem" [4]. Minimizing this tension requires a certain choice of the stop soft masses and the trilinear soft A-term [5], pointing to a "golden region" in the MSSM parameter space [6]. This region is characterized by fairly light stops (typically 300-400 GeV for $\tilde{t}_1$ and 500-800 GeV for $\tilde{t}_2$), and a large mixing angle θ_t (defined as the rotation angle from the gauge eigenbasis $\tilde{t}_L, \tilde{t}_R$

to the mass eigenbasis $\tilde{t}_1, \tilde{t}_2$). The shape of the golden region depends only weakly on the non-top sector MSSM parameters (within broad ranges of those parameters), and within the unrestricted MSSM this hypothesis is compatible with other interesting applications of SUSY such as dark matter [7]. If SUSY is discovered at the LHC, it would be very interesting to test whether the golden region hypothesis is realized.

There is a large body of literature on superpartner mass measurements at the LHC. (For example, ref. [8] studied stop mass determination in a framework similar to the one considered here.) The goal of this paper is to propose observables that are directly sensitive to the mixing angle θ_t. The basic idea is that this angle enters the stop-top-neutralino couplings. In particular, the amount of parity violation in these couplings is determined by θ_t (along with the neutralino mixing matrix). If the decay $\tilde{t} \to t\chi^0$ is kinematically allowed, this parity violation results in non-zero polarization of the tops produced in this decay. As is well known, tops decay before they hadronize, so that the top polarization is reflected in the angular distributions of the top decay products [10]. Observing these distributions can therefore provide information on θ_t. In this paper, we will show how such measurements can be performed at the LHC.[1]

The rest of the paper is organized as follows. In section 2, we discuss the connection between the stop mixing angle and the polarization of tops from $\tilde{t} \to t\chi^0$ decays in more detail, define the effective mixing angle which determines the degree of top polarization, and propose two observables which can be used to measure this effective angle. In section 3, we perform a parton-level analysis of the feasibility of the proposed measurements at the LHC, for a particular benchmark point (chosen to be compatible with the golden region) in the MSSM parameter space. The analysis includes the leading SM backgrounds, and we discuss a set of selection cuts to suppress these backgrounds to manageable levels. We project the sensitivity of the LHC experiments to the effective mixing angle with $10\,\text{fb}^{-1}$ of analyzed data. In section 4, we briefly discuss some of the issues involved in inferring the actual stop mixing angle θ_t from the measured effective angle. Finally, we present our conclusions and outline some questions for future study in section 5.

2 Polarized tops from stop decays

The stop mass terms in the MSSM Lagrangian have the form

$$\mathcal{L} = (t_L^*, t_R^*)\, M^2\, (t_L, t_R)^T\,, \tag{2.1}$$

where

$$M^2 = \begin{pmatrix} M_L^2 + m_t^2 + \Delta_u & \sqrt{2} m_t \sin\beta (A_t - \mu \cot\beta) \\ \sqrt{2} m_t \sin\beta (A_t - \mu \cot\beta) & M_R^2 + m_t^2 + \Delta_{\bar{u}} \end{pmatrix}, \tag{2.2}$$

and

$$\Delta_u = \left(\frac{1}{2} - \frac{2}{3}\sin^2\theta_W\right) \cos 2\beta\, m_Z^2\,, \qquad \Delta_{\bar{u}} = \frac{2}{3}\sin^2\theta_W\, \cos 2\beta\, m_Z^2\,. \tag{2.3}$$

[1] For an analysis of polarized top quarks from the decays of squarks produced in electron-positron collisions, see ref. [9].

The mass eigenstates $\tilde{t}_1$ and $\tilde{t}_2$ are superpositions of the gauge eigenstates, $\tilde{t}_L$ and $\tilde{t}_R$:

$$\begin{aligned}\tilde{t}_1 &= \cos\theta_t\,\tilde{t}_L + \sin\theta_t\,\tilde{t}_R\,,\\ \tilde{t}_2 &= -\sin\theta_t\,\tilde{t}_L + \cos\theta_t\,\tilde{t}_R\,,\end{aligned} \tag{2.4}$$

where the mixing angle is given in terms of the Lagrangian parameters by

$$\tan 2\theta_t = \frac{2\sqrt{2}m_t \sin\beta(A_t - \mu\cot\beta)}{M_L^2 - M_R^2 + \Delta_u - \Delta_{\bar{u}}}\,. \tag{2.5}$$

Since parity is violated in weak interactions, weak couplings of the stops depend on the angle θ_t. Of particular interest to us is the stop-top-neutralino coupling, since the parity asymmetry in this coupling can lead to non-vanishing polarization of top quarks produced in stop decays. Since the top quark decays before it hadronizes, this polarization is, at least in principle, observable. The relevant vertex has the form

$$g_{\rm eff}^{ij}\tilde{t}_i\tilde{\chi}_j^0\left(\cos\theta_{\rm eff}^{ij}\,P_L + \sin\theta_{\rm eff}^{ij}\,P_R\right)t\,, \tag{2.6}$$

where $j = 1\ldots4$ labels the neutralino mass eigenstates $\tilde{\chi}_j^0$, related to the gauge eigenstates $\tilde{N} = (\tilde{B}, \tilde{W}^3, \tilde{H}_d^0, \tilde{H}_u^0)$ by

$$\tilde{\chi}_j^0 = \sum_{k=1}^{4} N_{jk}\tilde{N}_k\,. \tag{2.7}$$

The effective mixing angles are given by

$$\begin{aligned}\tan\theta_{\rm eff}^{1j} &= \frac{y_t N_{j4}\cos\theta_t - \frac{2\sqrt{2}}{3}g' N_{j1}\sin\theta_t}{\sqrt{2}\left(\frac{g}{2}N_{j2} + \frac{g'}{6}N_{j1}\right)\cos\theta_t + y_t N_{j4}\sin\theta_t}\,,\\ \tan\theta_{\rm eff}^{2j} &= \frac{y_t N_{j4}\sin\theta_t + \frac{2\sqrt{2}}{3}g' N_{j1}\cos\theta_t}{\sqrt{2}\left(\frac{g}{2}N_{j2} + \frac{g'}{6}N_{j1}\right)\sin\theta_t - y_t N_{j4}\cos\theta_t}\,,\end{aligned} \tag{2.8}$$

where $y_t = \sqrt{2}m_t/(v\sin\beta)$. The main idea of this paper is that we may be able to get an unambiguous and fairly precise experimental measurement of one or more of the angles $\theta_{\rm eff}^{ij}$ at the LHC, by measuring the polarization of top quarks produced in the decay $\tilde{t} \to \tilde{\chi}^0 t$. If the neutralino mixing matrix is at least partly known from other measurements, this information can be used to extract (or at least constrain) θ_t. This information can in turn be used, together with the stop eigenmass measurements, to determine the stop-sector lagrangian parameters.

At the LHC, stops can be directly pair-produced by strong interactions, in the processes

$$pp \to \tilde{t}_i\tilde{t}_i^*. \tag{2.9}$$

Direct production of same-sign stop pairs is negligible. In addition, there may be a sizable sample of stops produced indirectly, namely in decays of other superpartners, particularly the gluino via $\tilde{g} \to t\tilde{t}$. (A brief discussion of the possibility of top polarization measurements in the gluino sample appeared in ref. [11].) Those events lead to more complicated final

JHEP03(2009)141

state topologies in the detector, and vetoing such topologies can be used to separate the "direct" and "indirect" stop samples. We will focus on the direct stop sample in this paper, assuming that the contamination from the indirect sample, if present, is negligible. This has the advantage of simpler events and more robust predictions, since the rate and event topologies in the indirect sample depend on many more MSSM parameters. Some of the analysis techniques described here could be applied to the indirect sample as well.

Once produced, stops will promptly decay. Possible two-body decay modes include $\tilde{t} \to t\tilde{\chi}^0$, $\tilde{t} \to b\tilde{\chi}^+$, $\tilde{t} \to W^+\tilde{b}$, and $\tilde{t} \to H^+\tilde{b}$. We are interested in the $\tilde{t} \to t\tilde{\chi}^0$ mode, which must be kinematically allowed and have a sizeable branching ratio for our analysis to apply. This decay is followed by $t \to W^+b$, and the W-boson then decays either hadronically (about 70% of events) or leptonically (about 10% for each lepton flavor). Angular distributions of the top decay products are sensitive to top polarization. For example, the angular distribution of the b quarks in the top rest frame has the form

$$\frac{d\sigma}{d\cos\hat{\theta}_b} \propto \left(\frac{m_t^2}{m_W^2}+2\right)(E_\chi + \sin 2\theta_{\rm eff} m_\chi) + \left(\frac{m_t^2}{m_W^2}-2\right) p_\chi \cos 2\theta_{\rm eff} \cos\hat{\theta}_b\,, \qquad (2.10)$$

where $\hat{\theta}_b$ is the angle between the momenta of the b quark and the neutralino coming from the same stop decay as the top, and E_χ and p_χ are the energy and momentum of this neutralino. (See appendix A.) In the case of hadronic W decay, the top rest frame can be reconstructed. The neutralino direction is unknown, since there is at least two missing energy particles in each event. However, since stops are heavy, in the reaction (2.9) they are produced close to threshold, so that the stops in the direct sample tend to not have large velocities in the lab frame. If the stop is at rest in the lab frame, the top and neutralino from the same stop decay are back-to-back in this frame. Then, the angle $\hat{\theta}_b$ is the same as θ_b, the angle between the b quark momentum in the top rest frame and the direction of the boost from this frame to the lab frame. The boost direction is simply the direction of the top momentum in the lab frame. The angle θ_b is experimentally measurable. As we show below, the distribution of events in this angle provides a useful polarization analyzer, even though the effect is washed out somewhat by the motion of the stops in the lab frame.

Another observable, useful for semileptonic top decays, is the angular distribution of the charged lepton. In the top rest frame it has the form

$$\frac{d\sigma}{d\cos\hat{\theta}_l} \propto E_\chi + \sin 2\theta_{\rm eff} m_\chi + p_\chi \cos 2\theta_{\rm eff} \cos\hat{\theta}_l\,. \qquad (2.11)$$

In semileptonic top decays, the missing neutrino does not allow for a reconstruction of the top rest frame. (Since there are other unobserved particles in the event, the two neutralinos, the neutrino energy and momentum cannot be reconstructed by imposing the W and top mass constraints.) However, one can define the "approximate" top rest frame in which $\mathbf{p}_b + \mathbf{p}_l = 0$, and the angular distribution of charged leptons in that frame can be used as a polarization analyzer, as will be shown below. Once again, we will use θ_l, the angle between the lepton momentum in the (approximate) top rest frame and the direction of the boost from this frame to the lab frame, as a stand-in for $\hat{\theta}_l$. This preserves most of the polarization asymmetry due to the low lab-frame velocities of directly produced stops.

JHEP03(2009)141

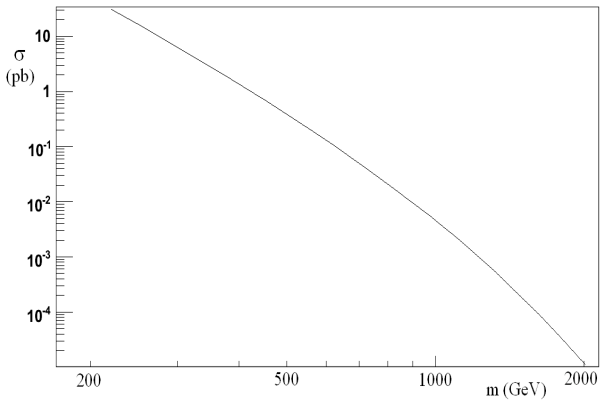

Figure 1. Leading-order cross section for $pp \to \tilde{t}\bar{t}^*$ at the LHC. We set the factorization and renormalization scales to $\mu = m_{\tilde{t}}$ and used the CTEQ6l1 parton distribution function set [16].

Note that t and $\bar{t}$ decays can be combined in the polarization analysis, since the polarization effects are the same for the two samples as a consequence of CP conservation.

3 Observability of top polarization at the LHC: a benchmark study

In this section, we demonstrate that top polarization in the stop pair-production sample can be observed and measured at the LHC. As with most effects in the MSSM, observability of top polarization, and the details of the analysis required to extract it from the data, depend on the choice of the MSSM parameters. We will perform a detailed analysis at a specific benchmark point in the MSSM parameter space, compatible with the golden region hypothesis of ref. [6].

3.1 Benchmark point and signature

We choose the following benchmark point (BP) in the MSSM parameter space (all parameters are specified at the weak scale):

$$\begin{aligned} M_1 = 100\,\text{GeV}, \qquad M_2 = M_3 = 1\,\text{TeV}\,; \qquad \mu = 400\,\text{GeV}, \qquad \tan\beta = 10; \\ m(\tilde{Q}_{1,2}) = m(\tilde{u}^c_{1,2}) = m(\tilde{d}^c_{1,2,3}) = m(\tilde{L}_{1,2,3}) = m(\tilde{e}^c_{1,2,3}) = 1\,\text{TeV}\,. \end{aligned} \tag{3.1}$$

All phases, flavor-violating couplings and masses, and all A-terms except for A_t, are set to zero. The three stop sector lagrangian patameters, $m(\tilde{Q}_3)$, $m(\tilde{u}^c_3)$, and A_t, determine the two stop eigenmasses, $M(\tilde{t}_1)$ and $M(\tilde{t}_2)$, and the mixing angle θ_t. In our analysis, we dial the lagrangian parameters to keep the stop masses fixed at

$$M(\tilde{t}_1) = 340\,\text{GeV}, \qquad M(\tilde{t}_2) = 800\,\text{GeV}\,, \tag{3.2}$$

while θ_t is varied to illustrate the analyzing power of the top polarization measurement. Note that the chosen stop eigenmasses, $\tan\beta$ and μ are compatible with the MSSM Golden Region, for values of θ_t sufficiently close to $\pi/4$ (maximal mixing).

JHEP03(2009)141

The cross section of direct stop-antistop pair production at the LHC, as a function of the stop mass, is shown in figure 1. At the BP, the cross sections are[2]

$$\begin{aligned}\sigma(pp \to \tilde{t}_1\tilde{t}_1^*) &= 3.23 \text{ pb}\,,\\ \sigma(pp \to \tilde{t}_2\tilde{t}_2^*) &= 33 \text{ fb}\,.\end{aligned} \tag{3.3}$$

The direct sample is completely dominated by $\tilde{t}_1$ pairs, and we will ignore the small $\tilde{t}_2$ contamination in our analysis. Moreover, all indirect stop production processes, such as gluino decays, are strongly suppressed at our BP; we will ignore those processes. The produced $\tilde{t}_1$ decays, with essentially 100% probability, via $\tilde{t}_1 \to t\chi_1^0$; all other two-body decays are kinematically forbidden. Thus, each event contains a top, an anti-top, and two neutralinos in the final state. Both hadronic and semileptonic top decays provide observables which can be used to infer top polarization. We will focus on the two angular distributions discussed in section 2, θ_b in hadronic top decays and θ_l for semileptonic tops. A priori, it is not clear which observable would provide better sensitivity in a realistic experiment: While the hadronic channel suffers from the finite resolution of the jet energy measurement and combinatoric backgrounds, the leptonic channel is limited by the inability to reconstruct the top rest frame in each event. We will explore this question by analyzing events where one of the tops decays hadronically and the other one semileptonically,[3] allowing us to study θ_b and θ_l distributions in the same sample. Thus, our final state is

$$t(3j) + \ell + j + \not{E}_T\,, \tag{3.4}$$

where $\ell = e, \mu$. An example of a Feynman diagram contributing to this final state is shown in figure 2. Other final states (two hadronic or two semileptonic tops) can also be considered, and we expect that some of the techniques discussed here will be applicable to those channels as well. However a detailed analysis is outside the scope of this paper.

3.2 SM backgrounds and cuts

Before presenting the polarization analysis, let us discuss the SM processes contributing to this final state, and propose a set of cuts that strongly suppress their contributions without materially affecting the polarization asymmetries in the signal.

Several SM processes contribute to the final state (3.4). The most important processes are listed in table 1. For concreteness, we will give cross sections with $\ell = \mu^+$.[4] The largest contribution by far comes from the $t\bar{t}$ channel, where one of the tops decays hadronically and

[2] All signal cross sections cited in this paper are evaluated at leading order, using CTEQ6l1 pdf set and setting the factorization and renormalization scale to the mass of the produced stop state. For the the $t\bar{t}$ background channels we set the factorization and renormalization scale to the top pole mass and for the W+jets events we use $\mu^2 = m_W^2 + \sum_{\text{jets}}(m_{tr}^2)$, where $m_{tr}^2 = m^2 + p_T^2$, summed over heavy quarks and light jets. We use the `MadGRAPH/MadEVENT` software package [12] to compute cross sections and generate events, except for the W+jets background channels, where we use `ALPGEN` [13].

[3] For a recent study of the LHC reach for stops and spin-1/2 top partners in this channel, see ref. [14].

[4] For the signal and the $t\bar{t}$ background channels, the cross sections with $\ell = e^-, e^+, \mu^-, \mu^+$ are identical. For the W+jets background channel, the cross sections with a negatively charged lepton are suppressed by about a factor of 2 compared to the ones shown in table 1.

JHEP03(2009)141

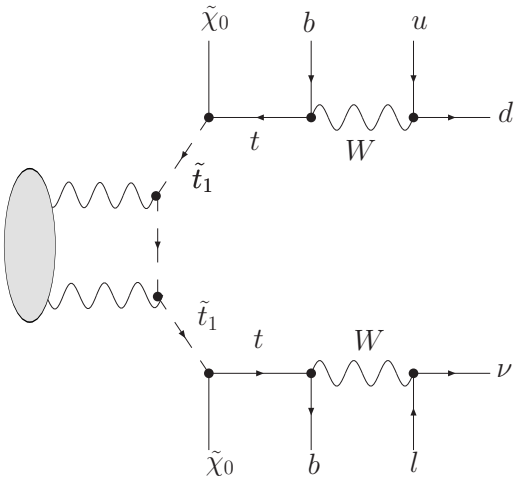

Figure 2. One of the diagrams contributing to the direct stop production in proton-proton collision, followed by the decay chain leading to the final state (3.4).

	σ_{tot}	$\sigma_{\text{tot}} \cdot \text{Br}$	$\sigma_{\text{tot}} \cdot \text{Br} \cdot \text{Eff}$	N_{sim}	Generator
$\tilde{t}_1\tilde{t}_1^*$ (BP)	3.23	0.18	0.014	8270	MG/ME
$t\bar{t}(\mu^+)$	550	29.2	$5.0 \cdot 10^{-3}$	$1.2 \cdot 10^6$	MG/ME
$t\bar{t}(\tau^+ \to \mu^+)$	550	2.42	$0.13 \cdot 10^{-3}$	$2.2 \cdot 10^5$	MG/ME
$2j + 2b + W^+$	101	3.7	$0.48 \cdot 10^{-3}$	$3.3 \cdot 10^5$	ALPGEN
$4j + W^+$	1330	132	$0.90 \cdot 10^{-3}$	$2.9 \cdot 10^5$	ALPGEN
Total BG	2531	167	$6.5 \cdot 10^{-3}$	$2.1 \cdot 10^6$	

Table 1. Signal and Background cross sections (in pb), before and after cuts. Also listed are the total number of events simulated for our study (including the b-tag efficiencies), and the software package used to generate the events.

the other one semileptonically. The semileptonic decays may produce μ^- directly or in a τ^- decay; we list the two contributions separately, to emphasize that the cut efficiencies for the two contributions differ due to their different kinematics. Another important background process is $4j + W$, where the invariant mass of three of the jets accidentally coincides with the top mass, and the W decays leptonically. In contrast, another obvious background, $t\bar{t}Z$, where the Z decays invisibly, has a very small cross section (only about 0.7 pb) and thus we will not include it in the analysis.

We generated and analyzed Monte Carlo event samples for the signal and each SM background roughly corresponding to $10\,\text{fb}^{-1}$ of integrated luminosity at the LHC. The simulations were performed using `MadGraph/MadEvent` (MG/ME) software package [12] except in the case of W+jets background, where we used the `ALPGEN` package [13]. The MG/ME simulations included integration over the phase space of the fully decayed final state (8-body final state in the case of signal, 6-body for the $t\bar{t}$ backgrounds). In the matrix element calculations, small-width approximation was not used, but only the Feynman

JHEP03(2009)141

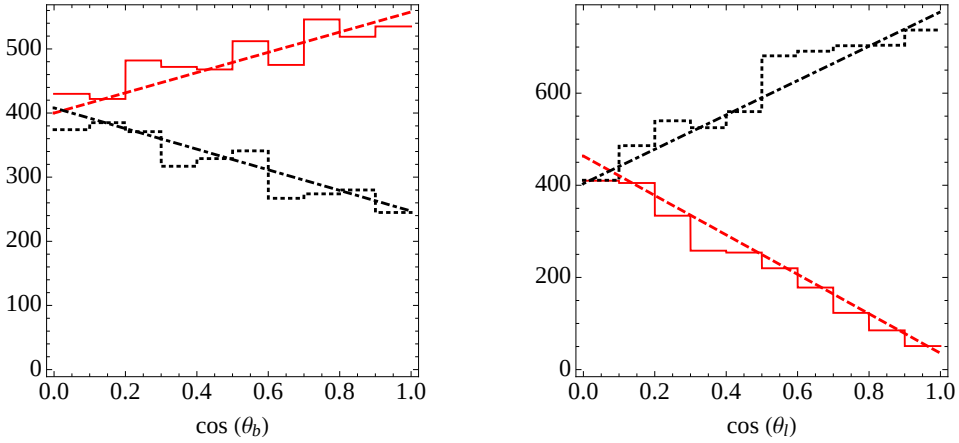

Figure 3. Comparison of the analytic predictions and events generated by `MadGraph/MadEvent` for the angular distribution of the b (left) and the charged lepton (right) in the top rest frame. Here $\hat{\theta}_b$ ($\hat{\theta}_l$) is the angle between the momenta of the b quark (charged lepton) and the neutralino coming from the same stop decay as the top. The solid (red) histogram corresponds to the Monte Carlo events with $\cos 2\theta_{\rm eff} = -1$ and the dashed (red) line corresponds to the analytic prediction. The dashed and dash-dotted (black) lines correspond to the MC distribution and analytic prediction, respectively, for $\cos 2\theta_{\rm eff} = +1$.

diagrams corresponding to the desired decay chain, such as the one shown in figure 2, were included. All polarization effects in the decay chains of interest are fully taken into account in this approximation. To verify this, we compared the simulated distributions in the angles $\hat{\theta}_b$ and $\hat{\theta}_l$ for the signal to the analytic predictions in eqs. (2.10), (2.11). The results are in excellent agreement, as shown in figure 3. Our analysis is restricted to the parton level; effects of hadronization, showering and intial state radiation are not included. To roughly model the detector response to jets and electrons, we introduce a Gaussian smearing of their energies according to [15]

$$\frac{\Delta E_j}{E_j} = \frac{50\%}{\sqrt{E_{\rm GeV}}} \oplus 3\%\,, \qquad \frac{\Delta E_e}{E_e} = \frac{10\%}{\sqrt{E_{\rm GeV}}} \oplus 0.7\%\,. \tag{3.5}$$

We do not apply smearing to muon energies, since the effect is small. To model the acceptance of the detector, we apply the following *acceptance cuts* at the generator level:

- $p_{T,j} > 25\,\text{GeV}$, $\eta \leq 4.0$ for each jet;
- $p_T^\ell \geq 20\,\text{GeV}$ and $\eta \leq 2.5$ for the charged lepton;
- $\Delta R(j_i, j_k) \geq 0.4$ for each jet pair, and $\Delta R(j_i, \ell) \geq 0.4$ for the charged lepton and each jet ($i, k = 1 \ldots 4$).

The results of our analysis are summarized in tables 1 and 2. The first column of table 1 lists, for reference, the total cross section of each process. For the $W+$ jets processes, the listed cross sections are computed imposing a cut $p_{T,j} > 20\,\text{GeV}$ on light (non-bottom)

JHEP03(2009)141

quarks and gluons. The second column of table 1 lists the cross sections to produce the final state (3.4) in each channel, including the above acceptance cuts. At this point, the signal is completely swamped by the $t\bar{t}$ background, with $S/B \sim 0.01$. To extract the signal, we impose the following *selection criteria*:

- At least one of the jets must be b-tagged. We assume energy-independent b-tag probabilities of 50% for a true b-jet, 10% for c-jet, and 1% for light quark and gluon jets.
- Large missing transverse energy: $\not{E}_T \geq 125\,\text{GeV}$.
- $\cos\phi(p_T^\ell, \not{E}_T) \leq 0.7$, where $\phi(p_T^\ell, \not{E}_T)$ is the opening angle between the transverse momentum of the charged lepton and the missing transverse momentum. This cut eliminates events where all missing energy comes from the leptonic decay of a highly boosted W.
- Hadronic Top Reconstruction (HTR): $\min|m_{3j} - m_t^{\text{true}}| \leq 5\,\text{GeV}$, where m_{3j} is the invariant mass of three jets, and the minimum is over the four possible triads. In our study, the true top mass m_t^{true} is taken to coincide with the value used in the MC generator, 172.5 GeV. The jet triad for which the minimum is achieved is identified with the hadronic top. This cut suppresses W+jets backgrounds.
- Semileptonic Top Veto (STV): Assuming that all missing energy comes from a massless neutrino, we reconstruct the candidate neutrino four-momentum $\bar{p}^\nu$ using the transverse $\not{E}_T$ measurement and the conditions $(\bar{p}^\nu)^2 = 0, (p^\ell + p^j + \bar{p}^\nu)^2 = m_t^2$, where p^j is the momentum of the jet which does *not* belong to the triad identified as the hadronic top. There are generically two solutions, $\bar{p}^\nu_{1,2}$. We then form $s_i^{\nu\ell} = (p^\ell + \bar{p}_i^\nu)^2$, and demand $\min_i|\sqrt{s_i^{\nu\ell}} - m_W| \geq 40\,\text{GeV}$. This cut suppresses the $t\bar{t}$ backgrounds, since the rejected kinematics corresponds to missing energy coming exclusively from semileptonic top decays.
- Separation Cuts (SC): $\Delta R(\ell^\pm, X) \leq 1.5$, where $\Delta R(\ell^\pm, X)$ is defined as the ΔR between the charged lepton and the jet closest to it in ΔR; and $0.8 \leq \Delta\bar{\phi}(\not{E}_T, X) \leq 1.3$, where $\Delta\bar{\phi}(\not{E}_T, X)$ is defined as the azimuthal angle between the $\not{E}_T$ vector and the object closest to it in ϕ. The signal and background distributions motivating these cuts are presented in figure 4.

The efficiencies of these cuts for the signal and each of the background samples are collected in table 2, and the cross sections after cuts for each process are listed in the third column of table 1. With these cuts, we obtain

$$S/B = 2.5; \quad S/\sqrt{B} = 36 \quad (\mathcal{L}_{int} = 10\ \text{fb}^{-1}). \tag{3.6}$$

Thus, we conclude that the stop signal is easily observable above the SM backgrounds after the selection cuts are imposed. We can then use this signal-dominated event sample for the polarization analysis.

JHEP03(2009)141

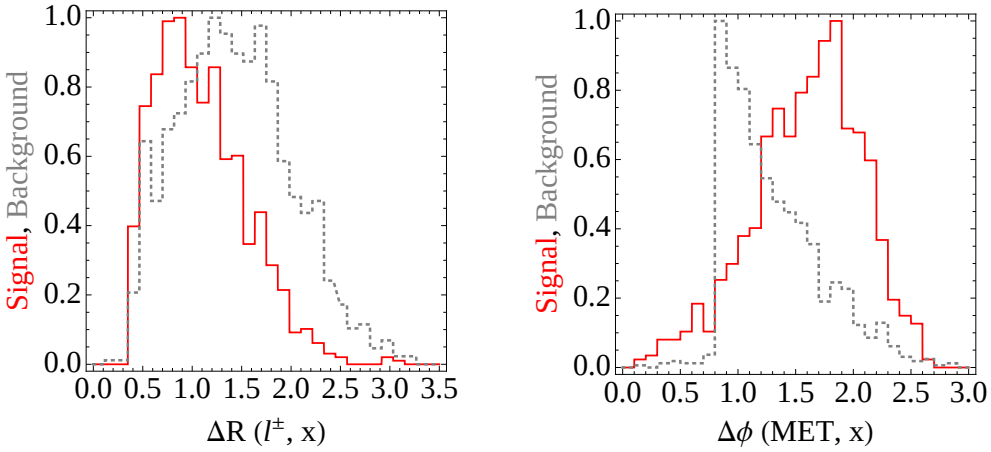

Figure 4. Normalized distributions in $\Delta R(\ell^{\pm}, X)$ and $\Delta\phi(\not{E}_T, X)$, in the signal and background samples satisfying all other acceptance and selection cuts. (See the text for the definition of the plotted observables.) The solid (red) line corresponds to the signal and the dotted (gray) line corresponds to the combined backgrounds.

	$\not{E}_T$	$\cos\phi(p_T^{\ell}, \not{E}_T)$	HTR	STV	SC	b-tag	Total
$\tilde{t}_1\tilde{t}_1^*$ (BP)	55	73	62	66	66	77	7.4
$t\bar{t}(\mu^-)$	8.2	37	63	7.7	26	77	0.025
$t\bar{t}(\tau^- \to \mu^-)$	17	7.4	61	5.2	7.1	77	$2.2 \cdot 10^{-3}$
$2j + 2b + W^-$	4.4	38	7.5	38	26	76	$4.4 \cdot 10^{-3}$
$4j + W^-$	3.0	38	8.2	37	24	5.1	$4.2 \cdot 10^{-4}$

Table 2. Selection cut efficiencies, in %. (Each cut is applied to the sample satisfying the acceptance cuts and all selection cuts listed above it in the text.)

Before proceeding, let us comment on the reliability of the Monte Carlo predictions for backgrounds, such as the $t\bar{t}$ simulation used in this study. Convincing interpretation of any excess over the SM background as contribution from new physics, in a situation where $S/B \sim 1$, would require precise understanding of the assumptions used in the background predictions. Since the LHC will produce a very large sample of $t\bar{t}$ pairs, the MC generators used to simulate this background can be precisely calibrated with data. This calibration can be done using samples which are not expected to suffer any SUSY contamination, such as the events with two reconstructed hadronic tops and small $\not{E}_T$. It can then be applied to samples where SUSY can contribute, e.g. events with large $\not{E}_T$ and a charged lepton which are our main focus here. It would be interesting to understand quantitatively the expected accuracy of such a validation procedure; such an analysis is however outside of the scope of this paper.

JHEP03(2009)141

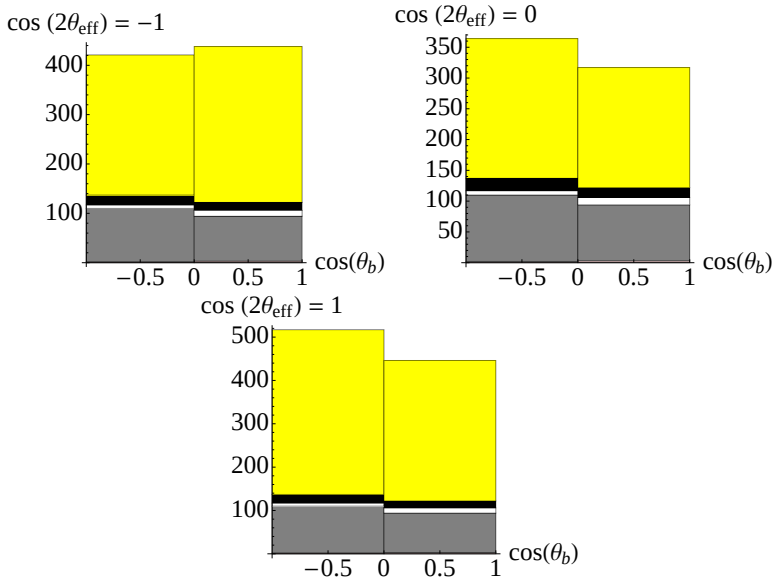

Figure 5. Angular distributions of events in the angle θ_b. The different contributions correspond to (from top to bottom): signal (yellow), $4j{+}W^-$ (black), $2j{+}2b{+}W^-$ (white), $t\bar{t}(\mu^-)$ (gray), $t\bar{t}(\tau^- \to \mu^-)$ (light red). The event numbers correspond to $10\,\mathrm{fb}^{-1}$ integrated luminosity at the LHC.

3.3 Polarization analysis

In section 2, we identified two observables, the angles θ_b and θ_l, which are potentially sensitive to the top polarization in the direct stop sample. The angle θ_b is the angle between the b jet in the jet triad identified as the hadronic top, and the direction of the hadronic top momentum, in the rest frame of the hadronic top. To define θ_l, we first define the approximate rest frame (ARF) of the semileptonic top, by adding the three-momenta of the charged lepton and the jet that does *not* belong to the reconstructed hadronic top. Then, θ_l is the angle, measured in the ARF, between the charged lepton and the direction of the ARF's motion with respect to the lab frame.

To measure the angle θ_b, we need to find which of the three jets in the hadronic top is the b jet. One way to do it would be to simply demand that one of the jets be b-tagged. An alternative method, which only relies on kinematics, is to compute the invariant masses of the three jet pairs inside the hadronic top, and to find the pair whose invariant mass is closest to m_W. The jet that does not belong to that pair can then be identified as the b jet. We found that in our sample the kinematic method has a higher efficiency than the simple b-tag, and thus we will use this technique to compute θ_b in each event.

In figures 5 and 6, we show the distribution of events in our Monte Carlo sample (signal and background, passing the above acceptance and selection cuts) in $\cos\theta_b$ and $\cos\theta_l$. The event numbers correspond to $10\,\mathrm{fb}^{-1}$ integrated luminosity at the LHC. Each figure shows the distributions for three values of θ_{eff}: from left to right, $\theta_{\mathrm{eff}} = 0, \pi/4, \pi/2$. The asymmetry due to top polarization is clearly visible in the distribution. One should note that, even though we were careful to choose selection cuts that have as little effect

JHEP03(2009)141

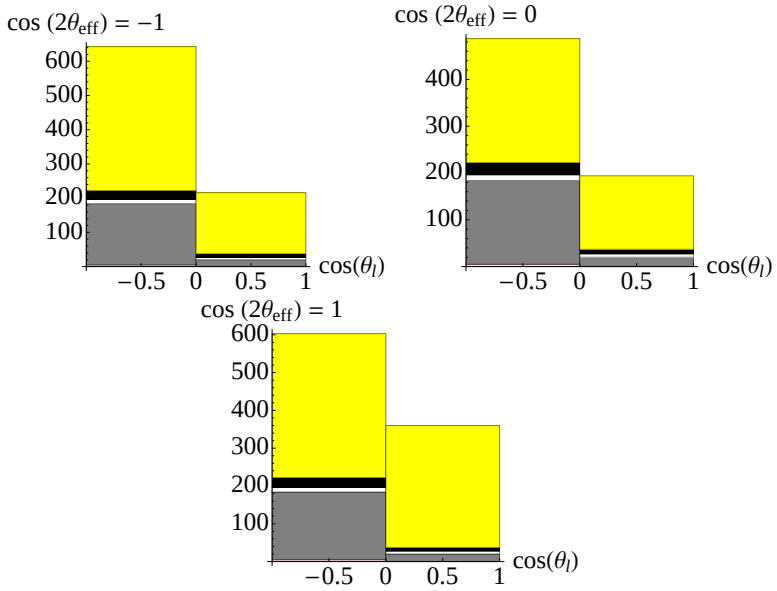

Figure 6. Angular distributions of events in the angle θ_l. The different contributions correspond to (from top to bottom): signal (yellow), $4j+W^-$ (black), $2j+2b+W^-$ (white), $t\bar{t}(\mu^-)$ (gray), $t\bar{t}(\tau^- \to \mu^-)$ (light red). The event numbers correspond to $10\,\mathrm{fb}^{-1}$ integrated luminosity at the LHC.

on the hadronic asymmetry as possible, the cuts do have a slight preference for the events with $\cos\theta_b < 0$, resulting in small asymmetries for the backgrounds and the signal at the parity-conserving point, $\theta_{\rm eff} = \pi/4$. Likewise, in the leptonic asymmetry, our use of the ARF instead of the true top rest frame leads to non-zero asymmetry in these cases. The important point, however, is that even though the measured asymmetry is not identical to the "primordial" asymmetry due to top polarization, there is still a simple one-to-one map between the two. To quantify the effect, we define two *forward-backward asymmetries (FBAs)*: The hadronic FBA is given by

$$A_{FB}^{\rm had} = \frac{\left(\int_0^1 - \int_{-1}^0\right) d\cos\theta_b \, \frac{d\sigma}{d\cos\theta_b}}{\left(\int_0^1 + \int_{-1}^0\right) d\cos\theta_b \, \frac{d\sigma}{d\cos\theta_b}}\,, \tag{3.7}$$

while the leptonic FBA is defined as

$$A_{FB}^{\rm lep} = \frac{\left(\int_0^1 - \int_{-1}^0\right) d\cos\theta_l \, \frac{d\sigma}{d\cos\theta_l}}{\left(\int_0^1 + \int_{-1}^0\right) d\cos\theta_l \, \frac{d\sigma}{d\cos\theta_l}}\,. \tag{3.8}$$

The statistical uncertainty of the FBA is given by

$$\Delta A_{FB} = 2\frac{\sqrt{N^+N^-}}{(N^+ + N^-)^{\frac{3}{2}}} \tag{3.9}$$

JHEP03(2009)141

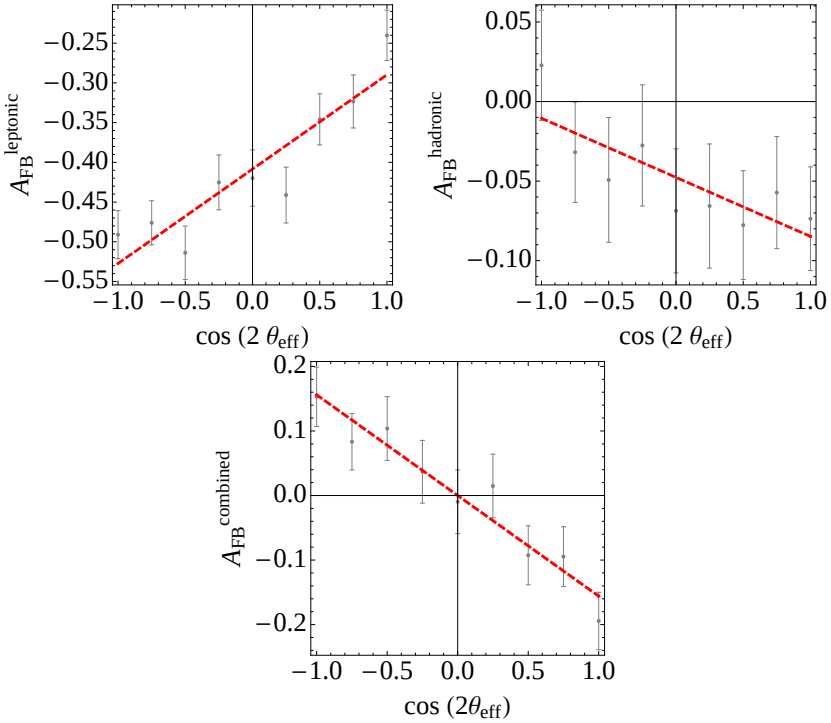

Figure 7. Leptonic, hadronic, and combined forward-backward asymmetries, as a function of the angle $\theta_{\rm eff}$. The error bars indicate statistical errors for $10\,{\rm fb}^{-1}$ integrated luminosity.

where $N^+ = \int_0^1 d\cos\theta_i \, \frac{d\sigma}{d\cos\theta_i}$ and N^- is the number of events in the opposite hemisphere. The combined asymmetry is defined as

$$A_{FB}^{\rm combined} \;=\; (A_{FB}^{\rm had} - A_{FB}^{\rm lep}) - \overline{(A_{FB}^{\rm had} - A_{FB}^{\rm lep})}\,, \tag{3.10}$$

where the second term signifies the average over the $\cos 2\theta_{\rm eff}$ values. For our MC event sample, we obtain

	$\theta_{\rm eff} = 0$	$\theta_{\rm eff} = \pi/4$	$\theta_{\rm eff} = \pi/2$
$A_{FB}^{\rm lep}$	-0.49 ± 0.03	-0.41 ± 0.03	-0.24 ± 0.03
$A_{FB}^{\rm had}$	0.022 ± 0.04	-0.069 ± 0.04	-0.074 ± 0.03
$A_{FB}^{\rm combined}$	0.15 ± 0.05	-0.01 ± 0.05	-0.19 ± 0.04

where the errors are statistical only, corresponding to $10\,{\rm fb}^{-1}$ worth of data at the LHC. We conclude that, at the level of our analysis, polarization effects in the stop direct sample are easily observable.

If the masses of $\tilde{t}_1$ and $\tilde{\chi}_1^0$ are measured independently, the measurement of the FBAs can be used to determine $\theta_{\rm eff}$. We studied the dependence of the hadronic and leptonic FBAs on $\theta_{\rm eff}$ by generating MC samples of the signal for 10 values of $\theta_{\rm eff}$, keeping all other MSSM parameters fixed at their BP values. The results are shown in figure 7.

JHEP03(2009)141

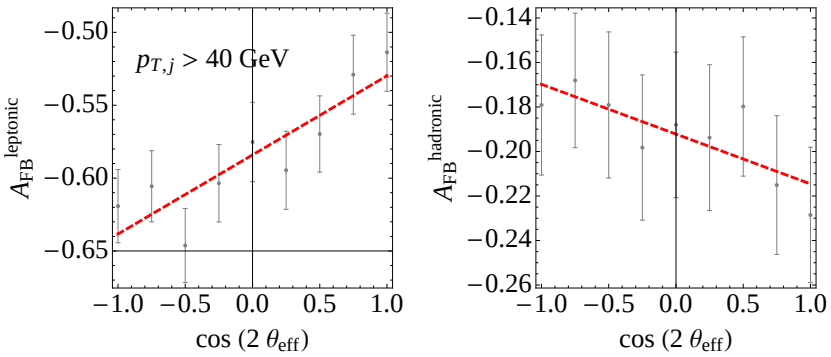

Figure 8. Leptonic and hadronic forward-backward asymmetries for $p_{T,j} > 40\,\text{GeV}$, as a function of the angle θ_{eff}. The error bars indicate statistical errors for $10\,\text{fb}^{-1}$ integrated luminosity.

The error bars indicate statistical errors for $10\,\text{fb}^{-1}$ integrated luminosity. As expected, we observe an approximately linear relationship between the asymmetries and $\cos 2\theta_{\text{eff}}$:

$$\begin{aligned} A_{FB}^{\text{lep}} &= +0.12\ \cos 2\theta_{\text{eff}} - 0.41\,, \\ A_{FB}^{\text{had}} &= -0.037\ \cos 2\theta_{\text{eff}} - 0.047\,, \\ A_{FB}^{\text{combined}} &= -0.16\ \cos 2\theta_{\text{eff}}\,. \end{aligned} \tag{3.11}$$

These formulas can be used to estimate the precision of θ_{eff} determination. Note, however, that the coefficients in these formulas depend on the stop and neutralino masses, and would need to be recalculated if these parameters differ from the BP values. The errors in the experimentally determined masses would need to be taken into account in the θ_{eff} determination.

Among the effects not included in our parton-level analysis, arguably the most important one is the absence of extra jets emitted as initial state radiation (ISR). Such jets would introduce a combinatoric background, making it more difficult to identify hadronic tops and potentially washing out the forward-backward asymmetries. The p_T distribution of the ISR jets is sharply peaked at zero, since most of these jets are soft or collinear with the incoming beams. An additional lower cut on the jet p_T (above the acceptance cut of $p_{T,j} \geq 20\,\text{GeV}$ assumed in the above analysis) may be necessary to suppress such jets. To estimate the sensitivity of our results to such a cut, we have repeated the analysis requiring $p_{T,j} \geq 40\,\text{GeV}$, keeping all other cuts the same. The results are presented in figure 8. It is clear that the hadronic asymmetry becomes essentially useless in this case, while the leptonic asymmetry is only marginally affected. The main effect of the additional $p_{T,j}$ cut on the leptonic asymmetry is in fact simply due to the reduced statistics, which can be overcome in time by increased integrated luminosity. Thus, we are optimistic that the leptonic asymmetry would survive as a useful observable even after the ISR and other showering, fragmentation and detector effects are included. Of course, a full detector-level analysis is needed to confirm this conclusion.

JHEP03(2009)141

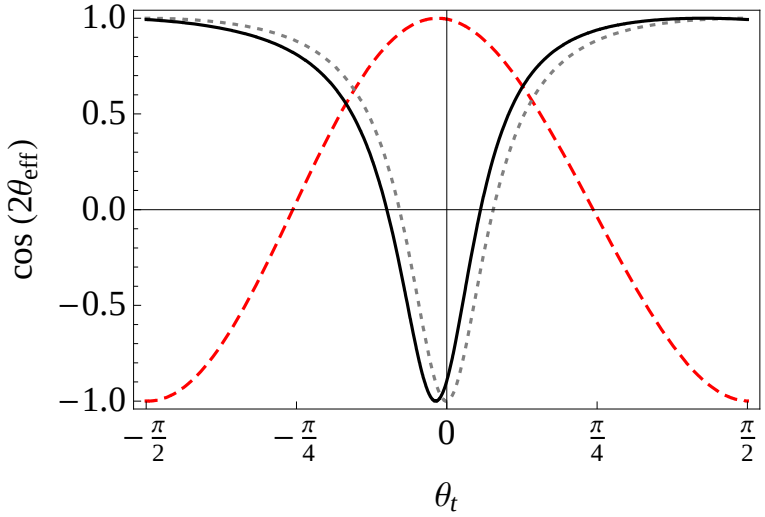

Figure 9. $\cos 2\theta_{\rm eff}$ vs. the stop mixing angle θ for three different neutralino mixing matrices. The solid (black) curve is our benchmark scenario, the dotted (gray) curve corresponds to the case where the lightest neutralino is pure bino and the dashed (red) curve corresponds to pure higgsino.

4 From top polarization to stop mixing

If the effective angle $\theta_{\rm eff}$ is measured using the technique described in the previous sections, the actual stop mixing angle can be found by inverting eq. (2.8):

$$\tan\theta_t = \frac{y_t N_{14}\cos\theta_{\rm eff} - \sqrt{2}\left(\frac{g}{2}N_{12} + \frac{g'}{6}N_{11}\right)\sin\theta_{\rm eff}}{y_t N_{14}\sin\theta_{\rm eff} + \frac{2\sqrt{2}}{3}g' N_{11}\cos\theta_{\rm eff}}\,. \tag{4.1}$$

Note, however, that several issues arise in this conversion. First, the top polarization observables measure $\cos 2\theta_{\rm eff}$, which introduces a two-fold degeneracy in the determination of θ_t. Secondly, in some cases, the mapping from $\cos 2\theta_{\rm eff}$ to θ_t introduces large errors even if $\cos 2\theta_{\rm eff}$ is precisely known: for example, this can occur for pure-bino neutralino if $\cos 2\theta_{\rm eff}$ is close to one, as seen in figure 2.8. Finally, to determine θ_t, one needs to know the composition of the lightest neutralino in terms of the gauge eigenstates. For example, in the cases of pure bino and pure higgsino, drastically different values of θ_t would be inferred from the same $\theta_{\rm eff}$ (see figure 2.8). In the case when the neutralino is predominantly a bino, it is especially important to independently constrain the subdominant contributions, since the $\tilde{H}\tilde{t}t$ and $\tilde{W}^3\tilde{t}t$ coupling constants are larger than the $\tilde{B}\tilde{t}t$ coupling, so that even a small higgsino or wino admixture can have a significant effect of $\theta_{\rm eff}$. Constraining the neutralino mixings at the level required to make the $\theta_{\rm eff} \to \theta_t$ conversion possible may in fact require substantially more integrated luminosity than the top polarization measurement itself. In spite of all these complications, this strategy seems to offer our best hope for the direct determination of the angle θ_t in the unconstrained MSSM framework, and is worth pursuing if SUSY is discovered.

JHEP03(2009)141

5 Discussion and conclusions

In this paper, we argued that top and anti-top quarks produced in stop decays in the MSSM are generically expected to be polarized, and that observing and measuring this polarization can provide information about the stop mixing angle. We proposed observables sensitive to top polarization, and illustrated the potential of the LHC to observe this effect, by performing a detailed study for a single benchmark point in the MSSM parameter space. We conclude that for the chosen benchmark point, the polarization effect should be observable with $10\,\mathrm{fb}^{-1}$ of data, and a useful measurement of the "effective" stop mixing angle θ_{eff} can be obtained. We also briefly discussed how the measurement of θ_{eff} can be used to constrain the actual stop mixing angle θ_t, one of the crucial parameters in assessing the naturalness of the EWSB in the MSSM.

The most important limitation of our analysis is that it is performed at the parton level, and only a very rough modeling of finite detector resolution by smearing jet and electron momenta was included. It is very important to perform a detector-level analysis including the effects of showering, hadronization and fragmentation, as well as detector effects. In particular, as we already remarked, ISR jets could contribute serious combinatoric backgrounds not included in this study, particularly for low-p_T jets. These backgrounds can be suppressed by tightening the minimum $p_{T,j}$ cut, and we have verified that at least one of our observables (the lepton asymmetry) appears to be rather insensitive to such tightening (see figures 7), (8). Still, it is important to analyze these issues quantitatively with a detector-level analysis.

Acknowledgments

We are grateful to Johannes Heinonen, Jay Hubisz, Mihoko Nojiri, Matthew Reece, Christian Spethmann and Gilad Perez for useful discussions. MP would like to thank the Institute for Physics and Mathematics of the Universe (IPMU) in Tokyo, and MP and AW would like to thank the Kavli Institute for Theoretical Physics (KITP) in Santa Barbara, where parts of this work were completed. AW is grateful to the Aspen Center of Physics where parts of this work were done. This research is supported by the NSF grant PHY-0355005.

Note Added. The main idea of this paper and some early results have been presented at the KITP Conference "Anticipating Physics at the LHC" in June 2008 [17]. Related ideas have also recently appeared in ref. [18].

A Observables sensitive to top polarization

The top quark decays before it hadronizes, and the information about its helicity is reflected in the distributions of the decay products. Consider the process $\tilde{t}_1 \to \tilde{\chi}_1^0 t$, followed by the decay of the top quark $t \to W^+ b$. The matrix element for this process is proportional to

$$\bar{u}(p_\chi)\ (\cos\theta_{\mathrm{eff}} P_L + \sin\theta_{\mathrm{eff}} P_R) \sum_{i=\pm} u_i(p_t)\bar{u}_i(p_t)\gamma^\mu P_L u(p_b)\epsilon_\mu(p_W)\,. \tag{A.1}$$

It is straightforward to calculate this matrix element in the coordinate system where the top quark is at rest, and the neutralino momentum is along the $+z$ axis. The non-zero matrix elements in the helicity basis are

$$\begin{aligned}
\mathcal{M}(\chi_+, W_0) &= \left(\cos\theta_{\text{eff}}\sqrt{E_\chi - p_\chi} + \sin\theta_{\text{eff}}\sqrt{E_\chi + p_\chi}\right) \cdot \frac{m_t}{m_W} \sin\frac{\theta}{2}\,, \\
\mathcal{M}(\chi_+, W_\perp) &= \left(\cos\theta_{\text{eff}}\sqrt{E_\chi - p_\chi} + \sin\theta_{\text{eff}}\sqrt{E_\chi + p_\chi}\right) \cdot \sqrt{2} \cos\frac{\theta}{2}\,, \\
\mathcal{M}(\chi_-, W_0) &= \left(\cos\theta_{\text{eff}}\sqrt{E_\chi + p_\chi} + \sin\theta_{\text{eff}}\sqrt{E_\chi - p_\chi}\right) \cdot \frac{m_t}{m_W} \cos\frac{\theta}{2}\,, \\
\mathcal{M}(\chi_-, W_\perp) &= \left(\cos\theta_{\text{eff}}\sqrt{E_\chi + p_\chi} + \sin\theta_{\text{eff}}\sqrt{E_\chi - p_\chi}\right) \cdot \sqrt{2} \sin\frac{\theta}{2}\,,
\end{aligned} \tag{A.2}$$

where E_χ and p_χ is the energy and momentum of the neutralino, θ is the angle between the b quark momentum and the z axis. The differential cross section is proportional to

$$\left(\frac{m_t^2}{m_W^2} + 2\right)(E_\chi + \sin 2\theta_{\text{eff}} m_\chi) + \left(\frac{m_t^2}{m_W^2} - 2\right) p_\chi \cos 2\theta_{\text{eff}} \cos\theta\,. \tag{A.3}$$

The presence of a term linear in $\cos\theta$ indicates parity violation, and measuring the size of this term provides information about the effective mixing angle θ_{eff}.

An analogous calculation for the leptonically decaying top results in a matrix element squared proportional to

$$|\mathcal{M}|^2 \propto E_\chi + \sin 2\theta_{\text{eff}} m_\chi + p_\chi \cos 2\theta_{\text{eff}} \cos\hat{\theta}_l\,. \tag{A.4}$$

Note that in both cases the magnitude of the neutralino momentum in the top rest frame is fixed because the neutralino is the final state of an effective two body decay.

References

[1] H.E. Haber and G.L. Kane, *The search for supersymmetry: probing physics beyond the standard model*, *Phys. Rept.* **117** (1985) 75 [SPIRES].

[2] S.P. Martin, *A supersymmetry primer*, hep-ph/9709356 [SPIRES].

[3] ALEPH collaboration, S. Schael et al., *Search for neutral MSSM Higgs bosons at LEP*, *Eur. Phys. J.* **C 47** (2006) 547 [hep-ex/0602042] [SPIRES].

[4] R. Barbieri and A. Strumia, *The "LEP paradox"*, hep-ph/0007265 [SPIRES].

[5] R. Kitano and Y. Nomura, *A solution to the supersymmetric fine-tuning problem within the MSSM*, *Phys. Lett.* **B 631** (2005) 58 [hep-ph/0509039] [SPIRES]; *Supersymmetry, naturalness and signatures at the LHC*, *Phys. Rev.* **D 73** (2006) 095004 [hep-ph/0602096] [SPIRES].

[6] M. Perelstein and C. Spethmann, *A collider signature of the supersymmetric golden region*, *JHEP* **04** (2007) 070 [hep-ph/0702038] [SPIRES].

[7] J. Kasahara, K. Freese and P. Gondolo, *Dark matter in the MSSM golden region*, *Phys. Rev.* **D 79** (2009) 045020 [arXiv:0805.0999] [SPIRES].

JHEP03(2009)141

[8] P. Meade and M. Reece, *Top partners at the LHC: spin and mass measurement*, *Phys. Rev.* **D 74** (2006) 015010 [hep-ph/0601124] [SPIRES].

[9] R. Kitano, T. Moroi and S.-f. Su, *Top-squark study at a future e^+e^- linear collider*, *JHEP* **12** (2002) 011 [hep-ph/0208149] [SPIRES].

[10] G.L. Kane, G.A. Ladinsky and C.P. Yuan, *Using the top quark for testing standard model polarization and CP predictions*, *Phys. Rev.* **D 45** (1992) 124 [SPIRES].

[11] J. Hisano, K. Kawagoe and M.M. Nojiri, *A detailed study of the gluino decay into the third generation squarks at the CERN LHC*, *Phys. Rev.* **D 68** (2003) 035007 [hep-ph/0304214] [SPIRES].

[12] *MadGraph/MadEvent v4* can be downloaded from http://madgraph.phys.ucl.ac.be/, for a discussion of the *Madgraph* project, see:
F. Maltoni and T. Stelzer, *MadEvent: automatic event generation with MadGraph*, *JHEP* **02** (2003) 027 [hep-ph/0208156] [SPIRES];
J. Alwall et al., *New developments in MadGraph/MadEvent*, *AIP Conf. Proc.* **1078** (2009) 84 [arXiv:0809.2410] [SPIRES].

[13] M.L. Mangano, M. Moretti, F. Piccinini, R. Pittau and A.D. Polosa, *ALPGEN, a generator for hard multiparton processes in hadronic collisions*, *JHEP* **07** (2003) 001 [hep-ph/0206293] [SPIRES].

[14] T. Han, R. Mahbubani, D.G.E. Walker and L.-T. Wang, *Top quark pair plus large missing energy at the LHC*, arXiv:0803.3820 [SPIRES].

[15] ATLAS collaboration, *ATLAS: Detector and physics performance technical design report. Volume 1*, SPIRES; *ATLAS detector and physics performance. Technical design report. Vol. 2*, SPIRES;
CMS collaboration, G.L. Bayatian et al., *CMS physics: technical design report*, SPIRES; *CMS technical design report, volume II: physics performance*, *J. Phys.* **G 34** (2007) 995 [SPIRES].

[16] J. Pumplin et al., *New generation of parton distributions with uncertainties from global QCD analysis*, *JHEP* **07** (2002) 012 [hep-ph/0201195] [SPIRES].

[17] http://online.kitp.ucsb.edu/online/lhc_c08/perelstein/oh/01.html.

[18] J. Shelton, *Polarized tops from new physics: signals and observables*, *Phys. Rev.* **D 79** (2009) 014032 [arXiv:0811.0569] [SPIRES].

JHEP03(2009)141